Flavor-changing neutral Higgs boson couplings and top-quark–charm-quark production at the Next Linear Collider

Wei-Shu Hou
Department of Physics, National Taiwan University, Taipei, Taiwan, Republic of China

Guey-Lin Lin
Institute of Physics, National Chiao Tung University, Hsinchu, Taiwan, Republic of China

Chien-Yi Ma
Department of Electrophysics, National Chiao-Tung University, Hsinchu, Taiwan, Republic of China

(Received 4 August 1997)

We explore the possibility of detecting flavor-changing neutral Higgs boson couplings at the Next Linear Collider (NLC) through $e^+e^-\to\nu_e\bar{\nu}_e t\bar{c}$. In the framework of a general two-Higgs-doublet model, we perform a complete calculation and find that $\sigma(e^+e^-\to\nu_e\bar{\nu}_e t\bar{c},\nu_e\bar{\nu}_e\bar{t}c)$ could reach ~ 9 fb for $\sqrt{s}=2$ TeV. This amounts to an annual production of 500 $t\bar{c}$ plus $\bar{t}c$ pairs at the NLC with an integrated luminosity of 50 fb^{-1}. The dependence of the tc-production rate on the neutral scalar mixing angle is mild except when $\sin^2\alpha\to 0$ or 1. The $\nu\nu W^+W^-$ background should be manageable after b tagging, while $\nu\nu t\bar{t}$ background should not be a problem when the signal event rate is still interesting. The process, together with $e^+e^-\to\nu_e\bar{\nu}_e W^+W^-,\nu_e\bar{\nu}_e ZZ$ studies, offer the chance of measuring the $t-c-$Higgs-boson coupling. [S0556-2821(97)07323-2]

PACS number(s): 14.80.Cp, 12.15.Ff, 13.90.+i, 14.65.Ha

I. INTRODUCTION

The mechanism for symmetry breaking and the fermion mass and mixing hierarchy pattern are the two remaining mysteries in the electroweak theory. The construction of high energy colliders such as the CERN Large Hadron Collider (LHC) and Next Linear Collider (NLC) are in fact aimed at resolving such mysteries. In this regard, the physical processes that should be studied thoroughly at such machines are those involving the top quark, whose properties have yet to be studied carefully, as well as the yet to be discovered Higgs boson(s).

It was suggested some time ago that [1], in multi-Higgs-doublet models, the ''natural'' flavor conservation condition [2] is not mandatory for the suppression of flavor-changing neutral current (FCNC) processes. Rather, Nature has provided its own cure: the existing hierarchical patterns in quark masses and mixing angles may imply a pattern for flavor-changing neutral Higgs-boson couplings (FCNH) that is consistent with low energy data [1]. An interesting consequence of this framework is the possibility of sizable $t-c-$neutral–Higgs-boson couplings which would have notable impact on top quark and Higgs physics [3,4]. To probe such couplings at colliders, several processes [5–7] have been proposed which can be studied at the NLC or LHC. At the NLC, one may look for $t\bar{c}$ pair production via $e^+e^-\to Z^*\to t\bar{c},\bar{t}c$ [5] (where the Z-t-c coupling is loop-induced), or like-sign top pair production via $e^+e^-\to h^0A^0\to tt\bar{c}\bar{c},\bar{t}\bar{t}cc$ [6]. At the LHC, such flavor nondiagonal couplings can be probed through the parton subprocess $cg\to tA^0\to tt\bar{c}$ [7], which involves the FCNH coupling directly in the production process.

Recently, Bar-Shalom *et al.* pointed out [8] that FCNH couplings may be probed at the NLC via the WW fusion process $e^+e^-\to\nu_e\bar{\nu}_e t\bar{c}$, $\nu_e\bar{\nu}_e\bar{t}c$, as shown in Fig. 1. With $\sqrt{s}=2$ TeV, and the masses of neutral Higgs bosons being 250 GeV and 1 TeV, respectively, they found $\sigma_{\nu\nu tc}\equiv\sigma(e^+e^-\to\nu_e\bar{\nu}_e t\bar{c})+\sigma(e^+e^-\to\nu_e\bar{\nu}_e\bar{t}c)\approx 5$ fb. Assuming an integrated luminosity of 50 fb^{-1} at the NLC, this implies an annual production of 125 $t\bar{c}$ and an equal number of $\bar{t}c$ pairs. The process has a much larger tc production rate than $e^+e^-\to Z^*\to t\bar{c}$, and does not suffer from s-channel suppression as $e^+e^-\to h^0A^0\to tt\bar{c}\bar{c}$. In view of this, we would like to follow up on this work. We shall perform a full calculation and compare with the effective W approximation used in Ref. [8], explore different scenarios for neutral Higgs masses, and clarify parameter dependence of the tc production cross section.

The paper is organized as follows. In Sec. II, we briefly review the two-Higgs-doublet model with FCNH couplings and present the result of a full calculation of $\sigma_{\nu\nu tc}$ using helicity methods. We then point out that $\sigma_{\nu\nu tc}$ is largest

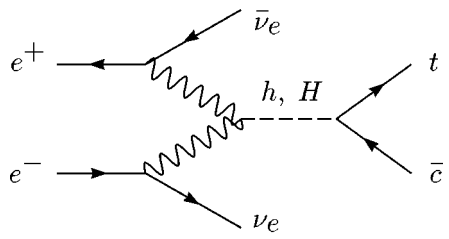

FIG. 1. Feynman diagram contributing to the process $e^+e^-\to\nu_e\bar{\nu}_e t\bar{c}$.

when both neutral scalars have mass of order the weak scale. This becomes the focus of our discussion throughout the paper. In Sec. III, we demonstrate the utility of the narrow width approximation. In Sec. IV we show that $\sigma_{\nu\nu tc}$ is not sensitive to the mixing angle of neutral scalars, and remains at the fb level for $\sqrt{s}\geqslant 1$ TeV. Some discussion of signal vs background is given. After concluding in Sec. V, we leave some technical details in Appendixes A and B.

II. FULL CALCULATION

The calculation of $\sigma_{\nu\nu tc}$ is based on the Lagrangian of a general two-Higgs-doublet model with flavor-changing neutral Higgs boson (FCNH) couplings

$$\begin{aligned}\mathcal{L}=&(D_\mu\Phi_1)^\dagger(D^\mu\Phi_1)+(D_\mu\Phi_2)^\dagger(D^\mu\Phi_2)-V(\Phi_1,\Phi_2)\\&-(\overline{u_L}M^u u_R+\overline{d_L}M^d d_R)\sqrt{2}\,\frac{\mathrm{Re}\phi_1^0}{v}\\&+(\overline{u_L}\xi^u u_R+\overline{d_L}\xi^d d_R)\sqrt{2}\,\mathrm{Re}\phi_2^0\\&+(-\overline{u_L}\xi^u u_R+\overline{d_L}\xi^d d_R)i\sqrt{2}\,\mathrm{Im}\phi_2^0\\&-\overline{d_L}V^\dagger\xi^u u_R\sqrt{2}\phi_2^-+\overline{u_L}V\xi^d d_R\sqrt{2}\phi_2^++\text{ H.c.},\end{aligned}\tag{1}$$

where $u_{L,(R)}$ and $d_{L,(R)}$ are flavor multiplets of up-type and down-type quarks, respectively, and $M^{u,d}$ are their diagonalized mass matrices. Note that we have relegated all the FCNH couplings to the second doublet as a result of rotating to the specific basis $\langle\phi_2^0\rangle=0$ and $\langle\phi_1^0\rangle=v/\sqrt{2}$ [9]. This is because there is no discrete symmetry [2] as in usual two-Higgs-doublet models [10] to distinguish between Φ_1 and Φ_2, so the familiar $\tan\beta\equiv v_1/v_2$ parameter is not physical. Assuming CP invariance in the Higgs sector, the scalar fields $\sqrt{2}\,\mathrm{Im}\phi_2^0$ and $\phi_2^\pm$ are identified as the physical pseudoscalar boson A^0 and charged scalar $H^\pm$. The CP even neutral scalars $\sqrt{2}\,\mathrm{Re}\phi_1^0$ and $\sqrt{2}\,\mathrm{Re}\phi_2^0$ can still mix through the Higgs potential $V(\Phi_1,\Phi_2)$ into the physical states H^0 and h^0. In the limit that the mixing angle $\sin\alpha\to 0$, $H^0\rightsquigarrow\sqrt{2}\,\mathrm{Re}\phi_1^0$ becomes the ''standard'' Higgs boson with diagonal couplings, while $h^0\rightsquigarrow\sqrt{2}\,\mathrm{Re}\phi_2^0$ has FCNH couplings characterized by the nondiagonal matrix $\xi_{ij}^{u,d}$.

In our calculation as well as in Ref. [8], the simple Cheng-Sher ansatz [1] is adopted:

$$\xi_{ij}^{u,d}=f_{ij}\frac{\sqrt{m_i m_j}}{v},\tag{2}$$

where f_{ij}'s are constants of order unity. The coupling ξ_{tc}^u is expected to be the largest and has the most prominent signature to be searched for in collider experiments. From Eq. (1), we can now single out the relevant couplings for computing the process $e^+e^-\to\nu_e\overline{\nu_e}t\overline{c}$, $\nu_e\overline{\nu_e}t\overline{c}$ given in Fig. 1. Since we wish to compare with Ref. [8], we take $f_{tc}\simeq\sqrt{2}$. The resulting $t-c-$Higgs-boson and Higgs-boson$-W-W$ couplings are

$$\begin{aligned}\mathcal{L}_{\mathrm{int}}=&\,g\frac{\sqrt{m_t m_c}}{\sqrt{2}m_W}(\sin\alpha H+\cos\alpha h)\,\overline{t\,c}\\&+\text{ H.c.}+gm_W(\cos\alpha H-\sin\alpha h)W^\mu W_\mu.\end{aligned}\tag{3}$$

The Higgs-boson$-Z-Z$ couplings can be easily incorporated, and the cross sections for $e^+e^-\to e^+e^-t\overline{c},e^+e^-\overline{t\,c}$ via ZZ fusion are simply related to that of $e^+e^-\to\nu_e\overline{\nu_e}t\overline{c}$, $\nu_e\overline{\nu_e}\,\overline{t\,c}$ [8].

A. Helicity amplitude calculation

A full calculation of $\sigma_{\nu\nu tc}$ is rather involved as the process considered is a $2\to 4$ scattering. An efficient way of doing it is by employing the helicity method [12], which facilitates the numerical manipulations of Feynman amplitudes.

The amplitude for $e^+(p_1)e^-(p_2)\to\overline{\nu_e}(p_3)\times\nu_e(p_4)t(p_t)\overline{c}(p_c)$ reads

$$\begin{aligned}i\mathcal{M}=&F[\overline{v}(p_1,\lambda_1)\gamma_\mu P_- v(p_3,\lambda_3)]\\&\times[\overline{u}(p_4,\lambda_4)\gamma^\mu P_- u(p_2,\lambda_2)][\overline{u}(p_t,\lambda_t)v(p_c,\lambda_c)]\\&\times\left[\frac{i}{q^2-m_H^2+im_H\Gamma_H}-\frac{i}{q^2-m_h^2+im_h\Gamma_h}\right]\\&\times\frac{-i}{(p_1-p_3)^2-m_W^2}\,\frac{-i}{(p_2-p_4)^2-m_W^2},\end{aligned}\tag{4}$$

where q is the momentum of the intermediate Higgs boson, $P_\pm\equiv(1\pm\gamma_5)/2$, and

$$F=\cos\alpha\,\sin\alpha\left(\frac{ig}{\sqrt{2}}\right)^2(igm_W)\left(ig\frac{\sqrt{m_t m_c}}{\sqrt{2}m_W}\right)\tag{5}$$

is a collection of coupling coefficients. Note that, except for the relative sign and differences in mass and width, the h and H contributions are basically the same. All fermion masses are set to zero except for the top quark, and the m_c dependence is kept only in the coupling of Eq. (2). The helicities of leptons are therefore completely fixed by their left-handed vector couplings to W bosons, i.e., $\lambda_1=\lambda_3=+$ and $\lambda_2=\lambda_4=-$. However, there are four combinations involving the helicities of top and charm quarks.

Let $A(\lambda_1,\lambda_3)\equiv\overline{v}(p_1,\lambda_1)\gamma_\mu P_- v(p_3,\lambda_3)$ and $B(\lambda_2,\lambda_4)\equiv\overline{u}(p_4,\lambda_4)\gamma^\mu P_- u(p_2,\lambda_2)$. One finds (see Appendix A for details)

$$\begin{aligned}A(++)&=\sqrt{2E_1}\sqrt{2E_3}\langle\hat{p}_3+|\gamma_{\mu-}|\hat{p}_1+\rangle,\\B(--)&=\sqrt{2E_2}\sqrt{2E_4}\langle\hat{p}_4-|\gamma_+^\mu|\hat{p}_2-\rangle,\end{aligned}\tag{6}$$

where $\omega_{\pm t}=\sqrt{E_t\pm|\vec{p}_t|}$, $\gamma_\pm^\mu$ are 2×2 matrices defined by $\gamma_\pm^\mu=(1,\mp\vec{\sigma})$, and $|\hat{p}\pm\rangle$ denote the two-component eigenvectors of the helicity operator $\vec{p}\cdot\vec{\sigma}/|\vec{p}|$, that is

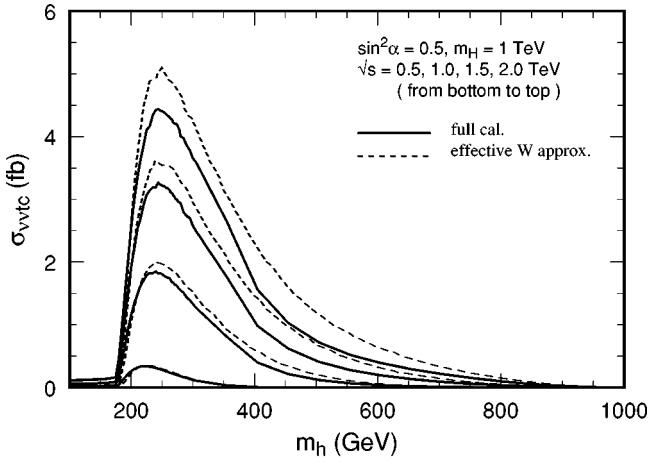

FIG. 2. The cross section $\sigma_{\nu\nu tc}$ as a function of m_h with $m_H=1$ TeV and $\sin^2\alpha=1/2$ for $s^{1/2}=0.5$, 1, 1.5, 2 TeV (bottom to top). Solid lines are for the full calculation, while dashed lines are from Ref. [8] which uses the effective W approximation.

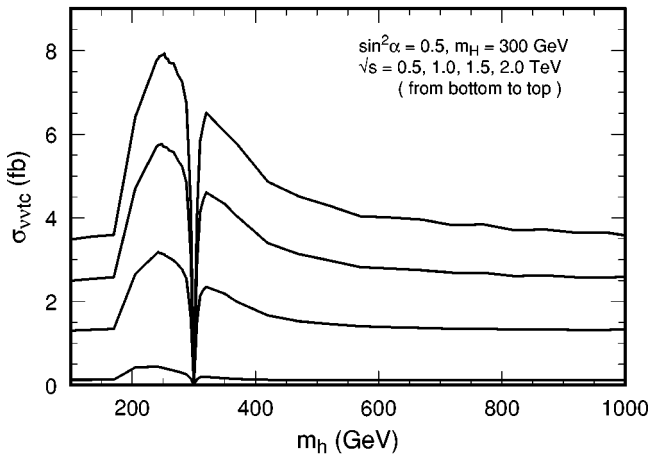

FIG. 3. The cross section $\sigma_{\nu\nu tc}$ as a function of m_h with $m_H=300$ GeV and $\sin^2\alpha=1/2$ for $s^{1/2}=0.5$, 1, 1.5, 2 TeV (bottom to top).

$$|\hat{p}+\rangle=\begin{pmatrix}\cos\dfrac{\theta}{2}\\ e^{i\phi}\sin\dfrac{\theta}{2}\end{pmatrix},\quad |\hat{p}-\rangle=\begin{pmatrix}-e^{-i\phi}\sin\dfrac{\theta}{2}\\ \cos\dfrac{\theta}{2}\end{pmatrix},\qquad (7)$$

where θ and ϕ are angles for $\vec{p}$. For the top-charm scalar density, define $C(\lambda_t,\lambda_c)\equiv\overline{u}(p_t,\lambda_t)v(p_c,\lambda_c)$, one gets four combinations (see Appendix A for details):

$$C(\mp\mp)=-\sqrt{2E_c}\,\omega_{+t}\langle\hat{p}_t\mp|\hat{p}_c\pm\rangle,$$

$$C(\mp\pm)=-\sqrt{2E_c}\,\omega_{-t}\langle\hat{p}_t\mp|\hat{p}_c\mp\rangle. \qquad (8)$$

Since $A(++)$ and $B(--)$ are already fixed, there are four helicity amplitudes $i\mathcal{M}(\lambda_t,\lambda_c)\propto C(\lambda_t,\lambda_c)$. With all four helicity amplitudes constructed, the subsequent numerical calculations can be done in a straightforward manner by utilizing the program ONETOP [12].

B. Comparison with Bar-Shalom *et al.*

To compare with Ref. [8], we compute $\sigma_{\nu\nu tc}$ for $m_H=1$TeV and $\sin^2\alpha=1/2$. The cross section $\sigma_{\nu\nu tc}$ as a function of m_h for $\sqrt{s}=$ 0.5, 1, 1.5, and 2 TeV are shown in Fig. 2. It peaks notably at $m_h\approx250$ GeV and decreases monotonously as m_h increases from 250 GeV. In accordance with the difference in the propagators given in Eq. (4), it vanishes in the degenerate limit $m_h=m_H=1$TeV. This is a special case for the choice of $\sin^2\alpha=1/2$ (i.e., $\alpha=\pi/4$), because the Higgs properties are identical in the degeneracy limit, so the amplitudes arising from each Higgs boson would then cancel completely. For $\sqrt{s}=2$ TeV, the maximal value of $\sigma_{\nu\nu tc}$ is around 4.5 fb, which is smaller than 5.2 fb obtained in Ref. [8] which uses the effective W approximation. Such an overestimation by the effective W approximation is a typical phenomenon in collider physics [11].

The prominent peaks in Fig. 2 suggest that the cross section arising from h alone would be the largest at $m_h\sim250$ GeV. Similar behavior should then be expected for the contribution from H. We therefore expect the total cross section resulting from H and h to be the largest *if both* m_H *and* m_h *are of order the weak scale*. This precisely fits the arguments given in Refs. [6,7] which emphasizes the mass range

$$200\ \text{GeV}<m_h,m_H<2m_t\approx350\ \text{GeV}. \qquad (9)$$

The lower bound is to allow the $t\bar{c}$ threshold to turn on. The upper bound of $2m_t\approx350$ GeV was imposed originally for the pseudoscalar A^0. For h and H, as can be seen from Fig. 2, the cross section is still sizable up to $m_{h,H}\cong500$ GeV for $\sqrt{s}>1$ TeV. This is because $\Gamma(h,H\to VV)\gg\Gamma(h,H\to f'\bar{f})$ for $m_{h,H}\sim350$ GeV, and the opening of $t\bar{t}$ mode does not increase substantially the total width of h or H. However, for the range of Eq. (9), the $t\bar{t}$ background to the $t\bar{c}$ or $\bar{t}c$ modes would be suppressed.

To show that $\sigma_{\nu\nu tc}$ is indeed more significant in the the range of Eq. (9), we show in Fig. 3 the cross section $\sigma_{\nu\nu tc}$ as a function of m_h for $m_H=300$ GeV and $\sin^2\alpha=1/2$. The cross section drops to zero at the degenerate limit $m_h=m_H=300$ GeV in a much more dramatic way. However, such a severe cancellation does not generally occur since there is no reason for m_h and m_H to be degenerate, and the cancellation is anyway incomplete for other values of $\sin\alpha$. The cancellation effect is negligible if the mass difference $\Delta M=|m_H-m_h|$ is a few times the widths of both Higgs bosons (see Appendix B). Slightly away from the degeneracy limit, the cross section rises to its peak value $\cong8.0$ fb at $m_h\approx250$ GeV for $\sqrt{s}=2$ TeV, which is almost twice as large as the case with $m_H=1$ TeV. As m_h increases to 1 TeV, $\sigma_{\nu\nu tc}$ drops to about 3.6 fb, which is mostly from H. For a lighter h, i.e., $m_h<250$ GeV, the cross section also drops. This once again illustrates the fact that $\sigma_{\nu\nu tc}$ receives the largest individual contributions from h and H respectively at $m_h,m_H\approx250$ GeV.

III. THE NARROW WIDTH APPROXIMATION

It is important to note that the widths of neutral Higgs boson in the mass range of Eq. (9), even up to ~500 GeV,

are still quite small compared to their masses. The standard model (SM) Higgs boson $H_{\rm SM}$ provides an upper bound to H and h widths, for example, $\Gamma_{H_{\rm SM}} \approx 15$ GeV for $m_{H_{\rm SM}}=350$ GeV [10]. Since the widths of both Higgs bosons are narrow in the mass range of interest, it is convenient to compute $\sigma_{\nu\nu tc}$ in the narrow width approximation. We may approximate $\sigma_{\nu\nu tc}$ by the cross section of Higgs boson production $\sigma(e^+e^-\to\overline{\nu_e}\nu_e h(H))$ multiplied by the branching ratio of the flavor-changing decay $h(H)\to t\overline{c}, \overline{t}c$. This approach is much simpler than the previous full calculation or even the effective W approximation. One can then determine the Higgs boson mass and $\sin^2\alpha$ dependences of $\sigma_{\nu\nu tc}$ with ease.

A. $WW\to h,H$ production

Compared to the previous calculation of $\sigma(e^+e^-\to\nu\overline{\nu t c})$, it is considerably simpler to compute the cross section $\sigma(e^+e^-\to\overline{\nu_e}\nu_e h(H))$. It is identical to that of SM Higgs boson production $\sigma(e^+e^-\to\overline{\nu_e}\nu_e H_{\rm SM})\equiv\sigma_{\nu\nu H_{\rm SM}}$ [10], except for the additional factors of $\cos^2\alpha$ or $\sin^2\alpha$. The amplitude for $e^+e^-\to\overline{\nu_e}\nu_e H_{\rm SM}$ is

$$\begin{aligned}\mathcal{M}(e^+(p_1)e^-(p_2)\to&\,\overline{\nu_e}(q_1)\nu_e(q_2)H_{\rm SM}(k))\\ &=\frac{ig^3 m_W}{8}\left(\frac{1}{2p_1\cdot q_1+m_W^2}\right)\\ &\times\left(\frac{1}{2p_2\cdot q_2+m_W^2}\right)[\overline{v}(p_1,s_1)\\ &\times\gamma^\mu(1-\gamma_5)v(q_1,s_2)][\overline{u}(q_2,s_4)\\ &\times\gamma_\mu(1-\gamma_5)u(p_2,s_3)]. \qquad (10)\end{aligned}$$

Averaging over the initial and summing over the final state spins give

$$\begin{aligned}\frac{1}{4}\sum_{\rm pol}|\mathscr{M}|^2=&\,g^6 m_W^2\left(\frac{1}{2p_1\cdot q_1+m_W^2}\right)^2\\ &\times\left(\frac{1}{2p_2\cdot q_2+m_W^2}\right)^2(p_2\cdot q_1)(p_1\cdot q_2), \qquad (11)\end{aligned}$$

where we have neglected fermion masses. The final state phase space integration is done by VEGAS [13]. For $\sqrt{s}=2$ TeV and $m_{H_{\rm SM}}=250$ GeV, we find $\sigma(e^+e^-\to\overline{\nu_e}\nu_e H_{\rm SM})\approx 264$ fb. The cross section for other values of m_H and $\sqrt{s}$ can be read off from Fig. 4.

B. $h,H\to t\overline{c}$ decay

To compute the branching ratio $B(h,H\to tc)$, we note that the dominant decay modes for $m_{h,H}<2m_t$ are $h,H\to W^+W^-$, ZZ, $b\overline{b}$ [10] and $t\overline{c}$, $\overline{t}c$ [3], where the latter are specific to the current model. The width of each decay mode is well known:

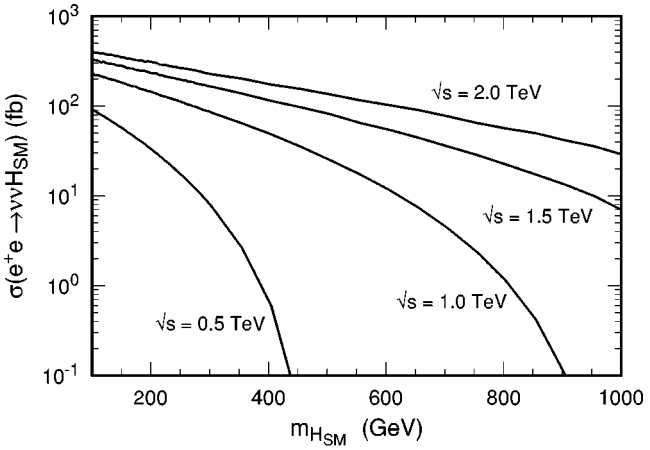

FIG. 4. The cross setion $\sigma_{\nu\nu H_{\rm SM}}$ of $e^+e^-\to\nu_e\overline{\nu_e}H_{\rm SM}$ as a function of $m_{H_{\rm SM}}$ for $s^{1/2}=0.5,\ 1,\ 1.5,\ 2$ TeV (bottom to top).

$$\Gamma(H\to W^+W^-)=\frac{g^2m_H^3}{64\pi m_W^2}\cos^2\alpha\sqrt{1-4x_W^2}(1-4x_W^2+12x_W^4),$$

$$\Gamma(H\to ZZ)=\frac{g^2m_H^3}{128\pi m_W^2}\cos^2\alpha\sqrt{1-4x_Z^2}(1-4x_Z^2+12x_Z^4),$$

$$\Gamma(H\to b\overline{b})\simeq\frac{3g^2m_H}{32\pi m_W^2}m_b^2(1-4x_b^2)^{3/2},$$

$$\Gamma(H\to t\overline{c}+\overline{t}c)=\left(\frac{f_{tc}}{\sqrt{2}}\right)^2\times\frac{3g^2m_H}{8\pi m_W^2}m_t m_c\times\sin^2\alpha(1-x_+^2)^{3/2}(1-x_-^2)^{1/2}, \qquad (12)$$

with $x_i=m_i/m_H$ and $x_\pm=(m_t\pm m_c)/m_H$. For $\Gamma(h\to W^+W^-,ZZ)$, etc. one simply changes $\sin^2\alpha\to\cos^2\alpha$. Note that we have assumed SM couplings for $b\overline{b}$, although it should depend on more parameters [this is another reason for the mass range of Eq. (9) so we avoid uncertainties in $H(h)$-t-$\overline{t}$ coupling]. However, the $b\overline{b}$ mode is unimportant for our purpose.

For a generic mixing angle α, vector boson decay modes dominate over the fermionic ones since the former is proportional to $m_{h,H}^3$ while the latter only depends on $m_{h,H}$ linearly. One can clearly see in Fig. 1 of Ref. [6] this severe suppression of $B(h,H\to tc)$ for generic α values [14]. However, for extreme values of $\alpha\to 0$ or 1, the WW, ZZ modes could be very suppressed, and either $B(h\to tc)$ or $B(H\to tc)$ become significant [6].

The threshold behavior of the $t\overline{c}$ mode and the dominance of h, $H\to WW$, ZZ modes in general help us understand the peak in $\sigma_{\nu\nu tc}$ at $m_{h,H}\approx 250$ GeV. We show in Fig. 5 the mass dependence of $B(h\to tc)$ for a few values of $\sin^2\alpha$ in the range

$$0.1<\sin^2\alpha<0.9. \qquad (13)$$

$B(H\to tc)$ can be simply obtained by making the change $\sin^2\alpha\to\cos^2\alpha$. We do not include extreme cases of $\sin^2\alpha\to 0$

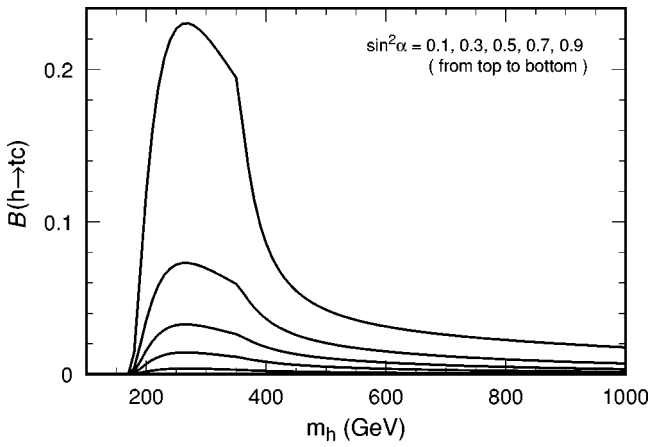

FIG. 5. The branching ratio $B(h\to tc)$ as a function of m_h for $\sin^2\alpha$=0.1,0.3,0.5,0.7,0.9 (top to bottom).

or 1 since $\sigma_{\nu\nu tc}\to 0$ in these limits. The shape of Fig. 5 can be understood as follows. $B(h,H\to tc)$ rises sharply right after the opening of the tc production threshold. The growth of $B(h,H\to tc)$ should however stop at certain Higgs boson mass, since $\Gamma(h,H\to VV)$ is in general dominant and grows more rapidly as $m_{h,H}$ increases. The peak position $m_{h,H}\cong 260$ GeV for $B(h,H\to tc)$, which is the main reason behind the peaks seen in Figs. 2 and 3, marks the point where the growth in $\Gamma(h,H\to tc)$ is overtaken by $\Gamma(h,H\to VV)$. It is interesting to note that $B(h,H\to tc)$ always peaks at $m_{h,H}\cong 260$ GeV independent of the $\sin^2\alpha$ we choose. This is easily understood since, for generic α, $B(H\to tc)\equiv\Gamma(H\to tc)/\Gamma_H\approx\Gamma(H\to tc)/\Gamma(H\to VV)$, i.e., $B(H\to tc)\approx\tan^2\alpha f(m_H)$ where $f(m_H)$ is largely α independent and peaks at $m_H\cong 260$ GeV. Similarly, we have $B(h\to tc)\approx\cot^2\alpha f(m_h)$. Such a simple dependence on the mixing angle α makes Fig. 5 very useful. For any $\sin^2\alpha$ in the range Eq. (13), one can obtain the branching ratio $B(h,H\to tc)$ for any Higgs boson mass by simply scaling via the relation $B(h,H\to tc)\approx\cot^2\alpha f(m_h^2)$, $\tan^2\alpha f(m_H^2)$.

We note that the kink due to $t\bar{t}$ threshold becomes more visible for small $\sin^2\alpha$ values. This is because the VV contribution to the Higgs boson width becomes suppressed and the relative weight of the $t\bar{t}$ contribution becomes more significant [15]. Such a kink is not apparent in Figs. 2 and 3 because the $\sin^2\alpha=1/2$ case was used.

C. Cross section

The SM Higgs boson width provides an upper bound to Γ_H and Γ_h. We can therefore use the narrow width approximation for $m_{H,h}<500$ GeV. The cross section $\sigma_{\nu\nu tc}$ can be written as

$$\sigma_{\nu\nu tc}\cong\sigma_{\nu\nu H_{\rm SM}}(m_{H_{\rm SM}}=m_H)\times\cos^2\alpha\times B(H\to tc)+\sigma_{\nu\nu H_{\rm SM}}(m_{H_{\rm SM}}=m_h)\times\sin^2\alpha\times B(h\to tc)+\text{interference terms},\tag{14}$$

where $H_{\rm SM}$ denotes the SM Higgs boson. Note that, with $|m_H^2-m_h^2|>(3-4)\times m_h\Gamma_h$, the interfernce term can be safely neglected (see Appendix B for details).

To locate the peak of $\sigma_{\nu\nu tc}$ for generic $\sin^2\alpha$, Eq. (14) can be rewritten as

$$\sigma_{\nu\nu tc}\cong\sigma_{\nu\nu H_{\rm SM}}(m_H)\times\sin^2\alpha\times f(m_H)+\sigma_{\nu\nu H_{\rm SM}}(m_h)\times\cos^2\alpha\times f(m_h),\tag{15}$$

where we have neglected the interference term by assuming a large enough splitting between m_H and m_h. With m_H and $\sin^2\alpha$ fixed as in the case of Figs. 2 and 3, $\sigma_{\nu\nu tc}$ only depends on $\sigma_{\nu\nu H_{\rm SM}}(m_h)\times f(m_h)$. Since $f(m_h)$ peaks at $m_h=260$ GeV and $\sigma_{\nu\nu H_{\rm SM}}$ is a monotonously decreasing function of $m_{H_{\rm SM}}$, the position of m_h giving maximal $\sigma_{\nu\nu tc}$ should be shifted downward from 260 GeV. This is exactly the case as seen in Figs. 2 and 3 where such effect are most significant for $\sqrt{s}=0.5$ TeV since $\sigma_{\nu\nu H_{\rm SM}}$ drops most steeply for increasing $m_{H_{\rm SM}}$ for this case. For $\sqrt{s}=2$ TeV, this shift becomes much smaller as $\sigma_{\nu\nu H_{\rm SM}}$ is relatively flat.

IV. DISCUSSION

To illustrate our arguments so far, let us explore the ''maximal'' and ''minimal'' $\sigma_{\nu\nu tc}$ cross sections in the mass range of Eq. (9), and $\sin\alpha$ and $\sqrt{s}$ dependences. We shall also make some general discussions about signal vs background and compare with other processes.

A. Range of cross sections

For ''maximal'' $\sigma_{\nu\nu tc}$, take, for example, $m_H=250$ GeV and $m_h=240$ GeV so $|m_H^2-m_h^2|\gtrsim 4\times m_h\Gamma_h$, and the interference term in $\sigma_{\nu\nu tc}$ can be safely neglected. Since the masses are approximately equal, one can rewrite Eq. (14) as

$$\sigma_{\nu\nu tc}\approx\sigma_{\nu\nu H_{\rm SM}}[\cos^2\alpha B(H\to tc)+\sin^2\alpha B(h\to tc)],\tag{16}$$

where the mass of $H_{\rm SM}$ can be taken as either that of H or h. Note that the combination $\cos^2\alpha B(H\to tc)+\sin^2\alpha B(h\to tc)$ determines the $\sin^2\alpha$ dependence of $\sigma_{\nu\nu tc}$, which is plotted in Fig. 6. It is interesting to see that both $\cos^2\alpha B(H\to tc)$ and $\sin^2\alpha B(h\to tc)$ are sensitive to $\sin^2\alpha$ but their sum is not. This is in large part because we chose almost equal m_H and m_h,

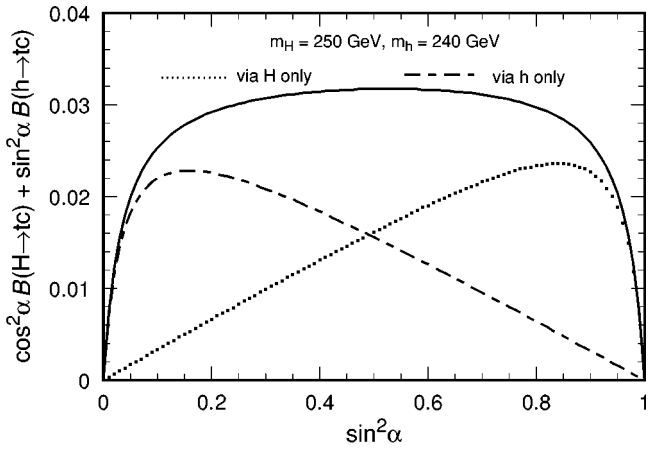

FIG. 6. The effective fraction $\cos^2\alpha B(H\to tc)+\sin^2\alpha B(h\to tc)$ as a function of $\sin^2\alpha$ with $m_H=250$ GeV and $m_h=240$ GeV.

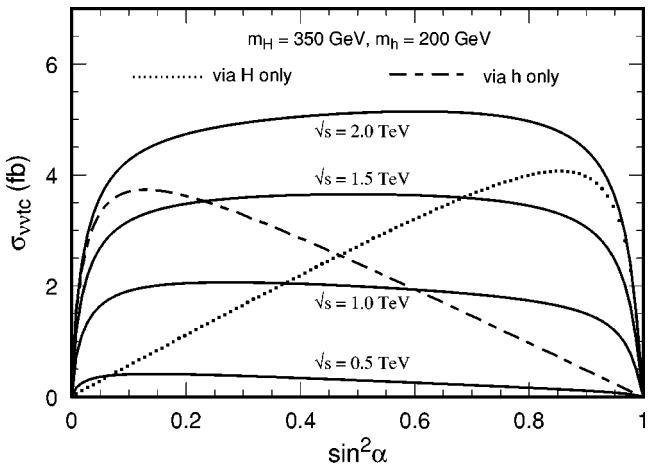

FIG. 7. The cross section $\sigma_{\nu\nu tc}$ as a function of $\sin^2\alpha$ with $m_H=350$ GeV and $m_h=200$ GeV for $s^{1/2}=0.5$, 1, 1.5, 2 TeV (bottom to top).

and reflects the mutually compensating nature between the two contributions. The effective fraction $\cos^2\alpha B(H\to tc)+\sin^2\alpha B(h\to tc)$ of the (''SM'') Higgs boson production cross section stays between 2–3 % for almost the entire range of $\sin^2\alpha$ of Eq. (13), but becomes extremely suppressed for $\sin^2\alpha$ outside this range.

For $\sqrt{s}=2$ TeV, $\sin^2\alpha=1/2$, and m_H, $m_h=250$, 240 GeV, from Figs. 4 and 6 we find

$$\sigma_{\nu\nu tc}\approx 270\ \text{fb}\times 3.2\%=8.6\ \text{fb}. \tag{17}$$

This is in good agreement with the maximal cross section obtained earlier from the full calculation, and illustrates the effectiveness of the narrow width approximation. The $\sin^2\alpha$ dependence is very mild. For example, at $\sin^2\alpha=0.1$ or 0.9, $\sigma_{\nu\nu tc}=6.8$ fb for $\sqrt{s}=2$ TeV, which is still comparable to the maximal cross section. The $\sin^2\alpha$ dependence for individual h or H contributions is much more significant.

To explore the ''minimal'' cross sections within the range of Eq. (9), we note from Figs. 2 and 3 that the contribution of h,H to $\sigma_{\nu\nu tc}$ is roughly equal for $m_{h,H}=200$ GeV and $m_{h,H}=350$ GeV. We therefore present the results for $m_H=350$ GeV and $m_h=200$ GeV, which gives roughly the smallest $\sigma_{\nu\nu tc}$ for the mass range of interest. We plot in Fig. 7 $\sigma_{\nu\nu tc}$ for this set of Higgs boson masses as a function of $\sin^2\alpha$ for $\sqrt{s}=0.5$, 1, 1.5, 2.0 TeV. It is seen that $\sin^2\alpha$ dependence remains mild. What is remarkable is that, *for almost all values of* $\sin^2\alpha$, $\sigma_{\nu\nu tc}$ *is at fb level or higher for* $\sqrt{s}\geq 1$ TeV. This promising result for $\sigma_{\nu\nu tc}$ holds only in the mass range given by Eq. (9), although the range can be extended up to $m_{h,H}\sim 400$–450 GeV or so.

In both Figs. 6 and 7 we have illustrated with cases where the h and H peak (in $\sin^2\alpha$) contributions are comparable, hence their $\sin^2\alpha$ dependences are mutually compensating. For more general choices of m_h and m_H values, some $\sin^2\alpha$ dependence would remain for $\sigma_{\nu\nu tc}$, which is reflected in and easily scaled from the individual h or H contributions.

B. Signal vs background

Turning to the experimental signal at the NLC, one needs to consider the final states from top quark decay, $t\to b\ell^+\nu$, bj_1j_2, hence the signal modes are

$$e^+e^-\to\nu_e\bar{\nu}_e t\bar{c}\to\nu_e\bar{\nu}_e\nu\ell^+b\bar{c},\ \ \nu_e\bar{\nu}_e b\bar{c}j_1j_2, \tag{18}$$

and similarly for $\nu_e\bar{\nu}_e\bar{t}c$. Since typical cross sections are a few fb in the mass range of Eq. (9), with an integrated luminosity of 50 fb^{-1}, we expect of order 100 or so (no more than 300) $\nu\nu bcj_1j_2$ events, and 1/6 of this in each $3\nu+\ell bc$ channels, where $\ell=e^\pm,\mu^\pm,\tau^\pm$. Although the event rates are significant, we find that the latter is not very promising once backgrounds are taken into account.

What are the potential backgrounds? Since the $\nu_e\bar{\nu}_e$ pair should carry away missing transverse energy $E_T\sim m_W$, WW fusion events should be relatively distinct at the NLC. For the mass range $m_{h,H}<2m_t$ of Eq. (9), background from $e^+e^-\to\nu_e\bar{\nu}_e h$, $\nu_e\bar{\nu}_e H\to\nu_e\bar{\nu}_e t\bar{t}$ is absent. The major background to be considered is therefore $e^+e^-\to\nu_e\bar{\nu}_e W^+W^-$ since it is more abundantly produced via h, $H\to W^+W^-$. From Figs. 4–7 one sees that $\sigma(e^+e^-\to\nu_e\bar{\nu}_e W^+W^-)$ is typically 20 to 30 times larger than the signal. But the important point to notice is that W decays do not contain b quarks ($<10^{-3}$ in B). The chief tool to suppress the WW background is therefore b tagging, expected to be very efficient at Linear Colliders [16]. However, since 1/3 of W decays contain charm quarks, fake rate of b tagging might be an issue. In particular, the $3\nu+\ell+bc$ mode would not be easy to distinguish from $3\nu+\ell+cs$ fakes when the signal event rate is so low. In contrast, the $\nu\nu bcj_1j_2$ mode has a second handle: kinematics and full reconstruction. With one b-tagged jet, two of the three remaining jets should reconstruct to m_W [17], and together with the b-jet reconstruct to a top quark. After such reconstruction, the signal events should show a mass peak over the WW background. Note that the WW ''background'' is itself the Higgs detection channel.

Of course, $t\bar{t}$ background would always be present. The $WW\to t\bar{t}$ scattering via t-channel b quark exchange is suppressed in phase space compared to $WW\to h$, H production followed by Higgs boson decay. When h, $H\to t\bar{t}$ threshold opens up (not until 400 GeV or so), one would have genuine $\nu\nu t\bar{t}\to\nu\nu+bb+4j$ background. These again can be distinguished from $\nu\nu tc$ production by event topology and jet counting. Since the $t\bar{t}/t\bar{c}$ ratio is not that large [3,8] up to $m_{h,H}\simeq 500$ GeV, they do not pose a major threat. However, as seen from Figs. 2 and 3, for Higgs boson mass beyond 400–450 GeV or so, the signal cross section has also become too low and the WW background itself may start to become serious.

C. Comparison of different processes

It is of interest to point out the difference between $\nu\nu tc$ production and other $t\bar{c}$ production processes. The $e^+e^-\to Z^*\to t\bar{c}$, $\bar{t}c$ [5] process, though rather clean, has very suppressed rate because the Z-t-c coupling is loop-induced [the Glashow-Iliopoulos-Maiani (GIM) mechanism

is intact in the present model context]. It is clear that $e^+e^- \to Z^* \to H(h)Z \to t\bar{c}\bar{Z}$ has identical $\sin^2\alpha$ dependence as the WW fusion process. However, this production mechanism is less promising since it suffers from s-channel suppression (cross section decreasing as $1/s$) at higher energies, and at the 500 GeV NLC, the rate is already a bit too low [6].

The $e^+e^- \to Z^* \to h(H)A$ process is also s-channel suppressed, hence it is not particularly interesting at higher energies. But it does offer the intriguing signal [6] of like-sign top quark pairs via $h(H)A \to tt\bar{c}\,\bar{c}, \bar{t}\,\bar{t}cc$, signaled by like-sign W plus $b\bar{b}$ events. Furthermore, the effects are the largest in this case when $\sin^2\alpha \to 0$ or 1, which is complementary to the $\sin^2\alpha$ domain of interest, Eq. (13), for the $e^+e^- \to \nu_e \bar{\nu}_e t\bar{c}$ process. At the 500–600 GeV NLC, the rates for the two processes are comparable, both leading to only a handful of clean events. Thus, though falling short of making a definitive study, the 500–600 GeV NLC can cover the full range of $\sin^2\alpha$ and offer us a glimpse of whether FCNH couplings exist or not.

Turning away from e^+e^- linear colliders, the process $\mu^+\mu^- \to h,H,A \to t\bar{c}$ [18] at a possible future muon collider capitalizes on the larger Higgs-boson$-\mu-\mu$ coupling and a sharp Higgs boson resonance peak. However, because of the narrow width of the Higgs boson, this would demand [6] precise tunings of the muon energies to find the Higgs boson resonance. In contrast, the beauty of the WW fusion process of Ref. [8] and discussed here is that no energy scan is necessary. It is not yet clear whether a high energy muon collider can be built or not [19].

Finally, let us compare with prospects at the LHC. The challenge for $VV \to h,\ H \to tc$ production search is the enormous background. It has been pointed out, however, that one might be able to *directly probe for FCNH coupling strengths* via the $cg \to tA \to tt\bar{c}$ production process at the LHC [7], which does not depend on $\sin\alpha$. Once again there is the intriguing signature of like-sign top quark pairs. The event rate is not very high since the raw cross section is at the 80 fb level [14], and one still needs to make event selection cuts. Although promising, background rejection would certainly still be a major issue, as is almost always the case for interesting new physics at hadron colliders. In contrast to the high rate environment of the LHC, however, all high p_T events at the NLC would be recorded and scrutinized. We stress that the search for FCNH effects via tc production is really part of the Higgs boson program. By studying the VV fusion processes alone, the relative large number of events in $\nu\nu tc$ mode (hundreds of events) and the concurrent study of Higgs boson properties via the W^+W^- and ZZ modes (thousands and hundreds of events, respectively) should allow one to measure the $h,H \to tc$ branching ratios, which in turn can lead to a determination of the FCNH coupling. Thus this has the advantage of being a complete program, and would be complementary to the $cg \to tA$ process at the LHC. However, since it would only be fruitful for $\sqrt{s} > 1$ TeV, the fulfillment of the program would certainly come *after* the studies at the LHC.

At any rate, we expect the study of $\nu\nu tc$ production via WW fusion to be quite feasible. We urge that a dedicated simulation study of this process for the NLC be carried out.

V. CONCLUSION

In summary, we have extended the work of Ref. [8] on tc production via $e^+e^- \to \nu_e \bar{\nu}_e tc$ at the NLC. We elucidate that the particularly promising mass range is when both m_h and m_H are of order the weak scale. This is quite different from the parameter range discussed by the authors of Ref. [8] where one of the Higgs bosons is taken to be as heavy as 1 TeV, and consequently the $\sigma_{\nu\nu tc}$ they obtained is smaller than ours. With Higgs-boson masses in the range of 200–350 GeV, we find that $\sigma_{\nu\nu tc}$ could reach almost 10 fb. The $\sin^2\alpha$ dependence is mild for $0.1 < \sin^2\alpha < 0.9$, and $\sigma_{\nu\nu tc}$ is greater than 1 fb as long as $\sqrt{s} \geq 1$ TeV. Given a significant cross section as such, this mode should be searched for carefully at future e^+e^- linear colliders such as the NLC.

ACKNOWLEDGMENTS

This work was supported in part by National Science Council of R.O.C. under Grant Nos. NSC 86-2112-M-002-019 and NSC 86-2112-M-009-012.

APPENDIX A: THE HELICITY METHOD

The helicity method is particularly suited for numerical manipulations of scattering amplitudes. For particles with spin, one constructs explicit representions for their helicity wave functions so that the relevant Feynman amplitudes can be written into numerical forms [12]. Consequently the squaring of scattering amplitudes may be performed numerically.

For fermions, we choose the Weyl basis with the following represention of γ matrices:

$$\gamma^0 = \begin{pmatrix} 0 & 1 \\ 1 & 0 \end{pmatrix}, \quad \gamma^j = \begin{pmatrix} 0 & -\sigma_j \\ \sigma_j & 0 \end{pmatrix}, \quad \gamma^5 = \gamma_5 = \begin{pmatrix} 1 & 0 \\ 0 & -1 \end{pmatrix}, \tag{A1}$$

or collectively

$$\gamma^\mu = \begin{pmatrix} 0 & \gamma_+^\mu \\ \gamma_-^\mu & 0 \end{pmatrix}, \tag{A2}$$

with $\gamma_\pm^\mu = (1, \mp\vec{\sigma})$. The chiral projection operator $P_\pm = (1 \pm \gamma_5)/2$ is then given by

$$P_+ = \begin{pmatrix} 1 & 0 \\ 0 & 0 \end{pmatrix}, \quad P_- = \begin{pmatrix} 0 & 0 \\ 0 & 1 \end{pmatrix}, \tag{A3}$$

where P_+ and P_- project onto upper and lower components of Dirac four-spinors.

In the Weyl basis, the Dirac spinor $u(\vec{p},\lambda)$ for a fermion with momentum $\vec{p}$ and helicity λ is given by

$$u(\vec{p},+) \equiv \begin{pmatrix} u_+(\lambda=+) \\ u_-(\lambda=+) \end{pmatrix} = \begin{pmatrix} \omega_+ |\hat{p}+\rangle \\ \omega_- |\hat{p}+\rangle \end{pmatrix},$$

$$u(\vec{p},-) \equiv \begin{pmatrix} u_+(\lambda=-) \\ u_-(\lambda=-) \end{pmatrix} = \begin{pmatrix} \omega_- |\hat{p}-\rangle \\ \omega_+ |\hat{p}-\rangle \end{pmatrix}, \tag{A4}$$

where $\omega_{\pm}=\sqrt{E\pm|\vec{p}|}$ and $|\hat{p}\pm\rangle$ denote the two-component eigenvectors of the helicity operator $h=\vec{p}\cdot\vec{\sigma}/|\vec{p}|$ with

$$|\hat{p}+\rangle=\begin{pmatrix}\cos\frac{\theta}{2}\\ e^{i\phi}\sin\frac{\theta}{2}\end{pmatrix},\quad |\hat{p}-\rangle=\begin{pmatrix}-e^{-i\phi}\sin\frac{\theta}{2}\\ \cos\frac{\theta}{2}\end{pmatrix}, \tag{A5}$$

where θ and ϕ are angles specifying the direction of $\vec{p}$: i.e.,

$$\vec{p}=|\vec{p}|(\sin\theta\cos\phi,\sin\theta\sin\phi,\cos\theta). \tag{A6}$$

Similarly, the spinors of antifermions in the Weyl basis are given by

$$v(\vec{p},+)\equiv\begin{pmatrix}v_+(\lambda=+)\\ v_-(\lambda=+)\end{pmatrix}=\begin{pmatrix}\omega_-|\hat{p}-\rangle\\ -\omega_+|\hat{p}-\rangle\end{pmatrix},$$

$$v(\vec{p},-)\equiv\begin{pmatrix}v_+(\lambda=-)\\ v_-(\lambda=-)\end{pmatrix}=\begin{pmatrix}-\omega_+|\hat{p}+\rangle\\ \omega_-|\hat{p}+\rangle\end{pmatrix}. \tag{A7}$$

We note that the helicity wave functions of spin 1 particles can be constructed out of the two building blocks: $|\hat{p}+\rangle$ and $|\hat{p}-\rangle$.

For any fermion(antifermion) line which contains arbitrary numbers of interaction vertices with bosons, the associated amplitude must be a linear combination of the structures

$$\overline{w_1}\cdots\gamma^\rho\gamma^\nu\gamma^\mu P_- w_2, \tag{A8}$$

and

$$\overline{w_1}\cdots\gamma^\rho\gamma^\nu\gamma^\mu P_+ w_2, \tag{A9}$$

where $w_1\equiv\binom{w_{1+}}{w_{1-}}$ and $w_2\equiv\binom{w_{2+}}{w_{2-}}$ can be either u or v. Note that, for simplicity, we do not specify the momentum and helicity dependence of the spinors. Using the Weyl representations of Dirac spinors and γ matrices, the above two structures are simplified into

$$w^\dagger_{1\pm}\cdots\gamma^\rho_+\gamma^\nu_-\gamma^\mu_+ w_{2-}, \tag{A10}$$

and

$$w^\dagger_{1\pm}\cdots\gamma^\rho_-\gamma^\nu_+\gamma^\mu_- w_{2+}, \tag{A11}$$

where the sign in the subscript of $w^\dagger_{1\pm}$ depends on the number of γ matrices inserted between the spinors. Using Eqs. (A4) and (A7), one can express Eqs. (A10) and (A11) as linear combinations of

$$\langle\hat{p}_1\pm|\cdots\gamma^\rho_+\gamma^\nu_-\gamma^\mu_+|\hat{p}_2\pm\rangle \tag{A12}$$

and

$$\langle\hat{p}_1\pm|\cdots\gamma^\rho_-\gamma^\nu_+\gamma^\mu_-|\hat{p}_2\pm\rangle. \tag{A13}$$

Defining the conjugate spinors as

$$|\widetilde{\hat{p}\pm}\rangle\equiv i\sigma_2(|\hat{p}\pm\rangle)^*, \tag{A14}$$

where

$$|\widetilde{\hat{p}+}\rangle=-|\hat{p}-\rangle,\quad |\widetilde{\hat{p}-}\rangle=+|\hat{p}+\rangle,$$

$$\langle\widetilde{\hat{p}+}|=-\langle\hat{p}-|,\quad \langle\widetilde{\hat{p}-}|=+\langle\hat{p}+|. \tag{A15}$$

Then, applying the relation

$$\sigma_2(\gamma^\alpha_\pm)^T\sigma_2=\gamma^\alpha_\mp, \tag{A16}$$

we have

$$\langle\hat{p}_1\pm|\cdots\gamma^\rho_+\gamma^\nu_-\gamma^\mu_+|\hat{p}_2\pm\rangle=\langle\widetilde{\hat{p}_2\pm}|\gamma^\mu_-\gamma^\nu_+\gamma^\rho_-\cdots|\widetilde{\hat{p}_1\pm}\rangle. \tag{A17}$$

and

$$\langle\hat{p}_1\pm|\cdots\gamma^\rho_-\gamma^\nu_+\gamma^\mu_-|\hat{p}_2\pm\rangle=\langle\widetilde{\hat{p}_2\pm}|\gamma^\mu_+\gamma^\nu_-\gamma^\rho_+\cdots|\widetilde{\hat{p}_1\pm}\rangle. \tag{A18}$$

We now apply the above formalism to calculate $e^+(p_1)e^-(p_2)\to\overline{\nu}_e(p_3)\nu_e(p_4)t(p_t)\overline{c}(p_c)$. First, the amplitude for this process has been written in Eq. (4) with its fermionic part denoted as $A\cdot B\cdot C$. The explicit forms of A, B, and C as shown in Eqs. (6) and (8) can be easily obtained by using Eqs. (A4)–(A18). Second, we note that the product $A\cdot B$ involves a contraction of Lorentz indices associated with matrices γ^μ_+ and $\gamma_{\mu-}$. Such contractions can be evaluated easily via the ''Fierz-like'' relation

$$(\gamma^\mu_+)_{ij}(\gamma_{\mu-})_{kl}=(\gamma^\mu_-)_{ij}(\gamma_{\mu+})_{kl}=2\delta_{il}\delta_{kj}, \tag{A19}$$

with i, j, k, and l being indices in spinor space. Indeed, from Eq. (A19), we have

$$\langle\hat{p}_3+|\gamma_{\mu-}|\hat{p}_1+\rangle\cdot\langle\hat{p}_4-|\gamma^\mu_+|\hat{p}_2-\rangle$$
$$=2\langle\hat{p}_3+|\hat{p}_2-\rangle\langle\hat{p}_4-|\hat{p}_1+\rangle. \tag{A20}$$

From Eqs. (4), (6), and (8) and Eq. (A20), one now has the full helicity amplitudes $iM(\lambda_t,\lambda_c)$ for $e^+(p_1)e^-(p_2)\to\overline{\nu}_e(p_3)\nu_e(p_4)t(p_t)\overline{c}(p_c)$, which can be easily incorporated into the numerical program ONETOP [12].

APPENDIX B: THE INTERFERENCE OF FEYNMAN AMPLITUDES

In this Appendix, we discuss the interference effects of scattering amplitudes arising from different neutral Higgs bosons. Let us use $i\mathcal{M}^S$ to denote the amplitudes of $e^+(p_1)e^-(p_2)\to\overline{\nu}_e(p_3)\nu_e(p_4)t(p_t)\overline{c}(p_c)$ contributions from neutral Higgs bosons $S=H$ and h. That is

$$i\mathcal{M}^S = i\mathcal{M}(e^+e^- \to \overline{\nu_e}\nu_e S^*(q))\frac{i}{q^2 - m_S^2 + im_S\Gamma_S} i\mathcal{M}(S^*(q) \to t\overline{c}), \tag{B1}$$

where $S^*(q)$ denotes the off-shell S with momentum q. The total cross section $\sigma_{\nu\nu t\bar{c}} \equiv \sigma(e^+(p_1) \times e^-(p_2) \to \overline{\nu_e}(p_3)\nu_e(p_4)t(p_t)\overline{c}(p_c))$ is given by

$$\sigma_{\nu\nu t\bar{c}} = \frac{(2\pi)^4}{2s}\int \frac{d^3\vec{p}_3}{(2\pi)^3 2E_3}\frac{d^3\vec{p}_4}{(2\pi)^3 2E_4}\frac{d^3\vec{p}_t}{(2\pi)^3 2E_t}\frac{d^3\vec{p}_c}{(2\pi)^3 2E_c}\delta^4(p_1+p_2-p_3-p_4-p_t-p_c)|i\mathcal{M}^H + i\mathcal{M}^h|^2. \tag{B2}$$

One can separate $\sigma_{\nu\nu t\bar{c}}$ into diagonal and interference terms, i.e.,

$$\sigma_{\nu\nu t\bar{c}} = \sigma^H_{\nu\nu t\bar{c}} + \sigma^h_{\nu\nu t\bar{c}} + \sigma^{H-h}_{\nu\nu t\bar{c}}. \tag{B3}$$

In the narrow width limit $\Gamma_{H(h)} \ll m_{H(h)}$, it is well known that

$$\sigma^{H(h)}_{\nu\nu t\bar{c}} = \sigma(e^+e^- \to \overline{\nu_e}\nu_e H(h)) \times B(H(h) \to t\overline{c}). \tag{B4}$$

However, the interference term $\sigma^{H-h}_{\nu\nu t\bar{c}}$ is more complicated. From Eqs. (B1)–(B3), we obtain

$$\begin{aligned}\sigma^{H-h}_{\nu\nu t\bar{c}} = &-\cos^2\alpha\,\sin^2\alpha\frac{(2\pi)^4}{2s}\int \frac{d^3\vec{p}_3}{(2\pi)^3 2E_3}\frac{d^3\vec{p}_4}{(2\pi)^3 2E_4}\frac{d^3\vec{q}}{(2\pi)^3}\int (2\pi)^3 dq^2 \frac{1}{2E_q}\delta^4(p_1+p_2-p_3-p_4-q)\\ &\times|i\mathcal{M}(e^+e^- \to \overline{\nu_e}\nu_e H_{\rm SM}^*(q))|^2\ 2\ {\rm Re}\left(\frac{1}{q^2 - m_H^2 + im_H\Gamma_H}\frac{1}{q^2 - m_h^2 - im_h\Gamma_h}\right)\int \frac{d^3\vec{p}_t}{(2\pi)^3 2E_t}\frac{d^3\vec{p}_c}{(2\pi)^3 2E_c}\\ &\times\delta^4(q - p_t - p_c)|i\mathcal{M}(H_{\rm SM}^*(q) \to t\overline{c})|^2,\end{aligned} \tag{B5}$$

where $E_q \equiv \sqrt{q^2 + \vec{q}^2}$, and $H_{\rm SM}^*(q)$ has been used to replace $H^*(q)$ or $h^*(q)$ since we have factored out the mixing-angle dependence $\cos^2\alpha\sin^2\alpha$.

In general, H and h are not degenerate. Without loss of generality, we may assume $m_H > m_h$ so that $m_H^2 - m_h^2 = L \times m_h\Gamma_h$ with $L > 0$. Furthermore let us take $x \equiv q^2 - m_H^2$. With a little algebra, the propagator part of Eq. (B5) can be written as

$$\begin{aligned}&\int\ (2\pi)^3 dq^2 \cdots 2\ {\rm Re}\left(\frac{1}{q^2 - m_H^2 + im_H\Gamma_H}\frac{1}{q^2 - m_h^2 - im_h\Gamma_h}\right)\cdots\\ &\quad = \int dx \frac{1}{2\pi}\cdots\left(\frac{1}{x^2 + m_H^2\Gamma_H^2} + \frac{1}{(x + Lm_h\Gamma_h)^2 + m_h^2\Gamma_h^2}\right)\\ &\qquad \times(2\pi)^4\cdots - \int dx \frac{1}{2\pi}\cdots\frac{(m_H^2\Gamma_H^2 - 2m_H\Gamma_H m_h\Gamma_h + (L^2+1)m_h^2\Gamma_h^2)}{(x^2 + m_H^2\Gamma_H^2)((x + Lm_h\Gamma_h)^2 + m_h^2\Gamma_h^2)}(2\pi)^4\cdots.\end{aligned} \tag{B6}$$

If H and h are precisely degenerate, i.e., $L = 0$, and $\sin^2\alpha = 1/2$ which implies $\Gamma_H = \Gamma_h$, the second term on the right-hand side of Eq. (B6) vanishes, while the first term eventually gives rise to $-(\sigma^H_{\nu\nu t\bar{c}} + \sigma^h_{\nu\nu t\bar{c}})$ which cancels completely the diagonal contributions as expected.

For $L \gtrsim 3$, we note that the $(L^2+1)m_h^2\Gamma_h^2$ term in Eq. (B6) already dominates over both $m_H^2\Gamma_H^2$ and $m_h^2\Gamma_h^2$, provided Γ_h^2 is not overly suppressed by too small a $\sin^2\alpha$. Therefore, in Eq. (B6), one may neglect the combination $m_H^2\Gamma_H^2 - 2m_H\Gamma_H m_h\Gamma_h$ with respect to $(L^2+1)m_h^2\Gamma_h^2$. In this approximation, one can show that the two terms on the right-hand side of Eq. (B6) lead to a vanishing interference term $\sigma^{H-h}_{\nu\nu t\bar{c}}$ in the narrow width limit of $\Gamma_{H(h)} \to 0$.

To see this, note that in the limit of $\Gamma_{H(h)} \to 0$, the dominant contributions to the x integration in Eq. (B6) comes from the vicinities of $x = -Lm_h\Gamma_h$ and $x = 0$. For $x \approx -Lm_h\Gamma_h$, we discard the term $1/(x^2 + m_H^2\Gamma_H^2)$ on the right-hand side of Eq. (B6) while the remaining terms are rearranged as follows:

$$\int dx \frac{1}{2\pi}\cdots\frac{1}{(x+Lm_h\Gamma_h)^2+m_h^2\Gamma_h^2}(2\pi)^4\cdots-\int dx\frac{1}{2\pi}\cdots\frac{(L^2+1)m_h^2\Gamma_h^2}{(x^2+m_H^2\Gamma_H^2)((x+Lm_h\Gamma_h)^2+m_h^2\Gamma_h^2)}(2\pi)^4\cdots$$

$$=\int dx\cdots\frac{1}{\pi}\frac{m_h\Gamma_h}{(x+Lm_h\Gamma_h)^2+m_h^2\Gamma_h^2}\frac{1}{2m_h\Gamma_h}(2\pi)^4\cdots;$$

$$-\int dx\cdots\frac{1}{\pi}\frac{(L^2+1)m_h^2\Gamma_h^2\cdot m_h\Gamma_h}{(x^2+m_H^2\Gamma_H^2)((x+Lm_h\Gamma_h)^2+m_h^2\Gamma_h^2)}\frac{1}{2m_h\Gamma_h}(2\pi)^4\cdots. \tag{B7}$$

In the limit $\Gamma_h\to 0$, the first term on the right-hand side of Eq. (B7) can be simplified by

$$\frac{1}{\pi}\frac{m_h\Gamma_h}{(x+Lm_h\Gamma_h)^2+m_h^2\Gamma_h^2}\to\delta(x+Lm_h\Gamma_h), \tag{B8}$$

while the factor $1/2m_h\Gamma_h$ leads to $B(h\to tc)$ when combined with other terms in Eq. (B5). Similarly, the second term on the right-hand side of Eq. (B7) can be simplified by

$$\frac{1}{\pi}\frac{(L^2+1)m_h^2\Gamma_h^2\cdot m_h\Gamma_h}{(x^2+m_H^2\Gamma_H^2)((x+Lm_h\Gamma_h)^2+m_h^2\Gamma_h^2)}\to\frac{(L^2+1)m_h^2\Gamma_h^2}{(L^2m_h^2\Gamma_h^2+m_H^2\Gamma_H^2)}\delta(x+Lm_h\Gamma_h)$$

$$\simeq\delta(x+Lm_h\Gamma_h), \tag{B9}$$

where we have used $L^2\gg 1$. Clearly the two terms on the right-hand side of Eq. (B7) cancel completely, hence $\sigma^{H-h}_{\nu\nu t\bar{c}}$ receives no contribution from $x\approx -Lm_h\Gamma_h$. By similar arguments the integration region $x\approx 0$ also gives no contributions to $\sigma^{H-h}_{\nu\nu t\bar{c}}$. We therefore conclude that $\sigma^{H-h}_{\nu\nu t\bar{c}}=0$ provided we neglect the combination $m_H^2\Gamma_H^2-2m_H\Gamma_H m_h\Gamma_h$ with respect to $(L^2+1)m_h^2\Gamma_h^2$. Keeping the $m_H^2\Gamma_H^2-2m_H\Gamma_H m_h\Gamma_h$ term in Eq. (B6), the resulting $\sigma^{H-h}_{\nu\nu t\bar{c}}$ is at least $O(1/L^2)$ suppressed compared to the total diagonal cross section $(\sigma^{H}_{\nu\nu t\bar{c}}+\sigma^{h}_{\nu\nu t\bar{c}})$.

[1] T. P. Cheng and M. Sher, Phys. Rev. D **35**, 3484 (1987).

[2] S. L. Glashow and S. Weinberg, Phys. Rev. D **15**, 1958 (1977).

[3] W.-S. Hou, Phys. Lett. B **296**, 179 (1992).

[4] L. J. Hall and S. Weinberg, Phys. Rev. D **48**, R979 (1993).

[5] D. Atwood, L. Reina, and A. Soni, Phys. Rev. D **53**, 1199 (1996).

[6] W.-S. Hou and G.-L. Lin, Phys. Lett. B **379**, 261 (1996).

[7] W.-S. Hou, G.-L. Lin, C.-Y. Ma, and C.-P. Yuan, Phys. Lett. B **409**, 344 (1997).

[8] S. Bar-Shalom, G. Eilam, A. Soni, and J. Wudka, Phys. Rev. Lett. **79**, 1217 (1997).

[9] M. Luke and M. J. Savage, Phys. Lett. B **307**, 387 (1993).

[10] For a general review of Higgs boson physics, see J. F. Gunion *et al.*, *The Higgs Hunter's Guide* (Addison-Wesley, Reading, MA, 1990).

[11] For discussions of the effective W approximation, see the TASI-94 lectures of S. Dawson, *Introduction to the Physics of Higgs Bosons*, proceedings (World Scientific, Singapore, 1995).

[12] D. Carlson and C.-P. Yuan, the Monte-Carlo Event Generator ONETOP, Version 2.00, 1994; D. Carlson, Ph.D. thesis, Michigan State University, 1995. We thank C.-P. Yuan for a copy of the ONETOP code.

[13] G. P. Lepage, J. Comput. Phys. **27**, 192 (1978).

[14] We note that numerical results of Refs. [6] and [7] were given in the convention of $f_{tc}=1$, while we have taken $f_{tc}=\sqrt{2}$ in the current paper for sake of comparison with Ref. [8].

[15] Compare Fig. 2 of Ref. [3], which studies the case of $h\to t\bar{c}$ vs $h\to t\bar{t}$ in the limit $\sin^2\alpha\to 0$, when WW and ZZ modes are absent.

[16] T. Tauchi, plenary talk at *3rd Workshop on Physics and Experiments with Linear Colliders (LCWS 95)*, edited by A. Miyamoto *et al.* (World Scientific, Singapore, 1996).

[17] R. Frey, plenary talk at *3rd Workshop on Physics and Experiments with Linear Colliders (LCWS 95)* (Ref. [16]).

[18] D. Atwood, L. Reina, and A. Soni, Phys. Rev. Lett. **75**, 3800 (1995).

[19] See, for example, Mu^+Mu^+ *Colliders*, Proceedings of the Symposium on Physics Potential and Development of $\mu^+\mu^-$ Colliders, San Francisco, California 1995, edited by D. Cline [Nucl. Phys. B (Proc. Suppl.) **51A** (1996)].